

We are IntechOpen, the world's leading publisher of Open Access books Built by scientists, for scientists

6,900

Open access books available

186,000

International authors and editors

200M

Downloads

Our authors are among the

154

Countries delivered to

TOP 1%

most cited scientists

12.2%

Contributors from top 500 universities



WEB OF SCIENCE™

Selection of our books indexed in the Book Citation Index
in Web of Science™ Core Collection (BKCI)

Interested in publishing with us?
Contact book.department@intechopen.com

Numbers displayed above are based on latest data collected.
For more information visit www.intechopen.com



Chapter

Development of a Fatigue Life Assessment Model for Pairing Fatigue Damage Prognoses with Bridge Management Systems

*Timothy Saad, Chung C. Fu, Gengwen Zhao
and Chaoran Xu*

Abstract

Fatigue damage is one of the primary safety concerns for steel bridges reaching the end of their design life. Currently, US federal requirements mandate regular inspection of steel bridges for fatigue cracks; however, these inspections rely on visual inspection, which is subjective to the inspector's physically inherent limitations. Structural health monitoring (SHM) can be implemented on bridges to collect data between inspection intervals and gather supplementary information on the bridges' response to loads. Combining SHM with finite element analyses, this paper integrates two analysis methods to assess fatigue damage in the crack initiation and crack propagation periods of fatigue life. The crack initiation period is evaluated using S-N curves, a process that is currently used by the FHWA and AASHTO to assess fatigue damage. The crack propagation period is evaluated with linear elastic fracture mechanic-based finite element models, which have been widely used to predict steady-state crack growth behavior. Ultimately, the presented approach will determine the fatigue damage prognoses of steel bridge elements and damage prognoses are integrated with current condition state classifications used in bridge management systems. A case study is presented to demonstrate how this approach can be used to assess fatigue damage on an existing steel bridge.

Keywords: fatigue, fatigue damage, structural health monitoring, damage prognoses, fatigue assessment, bridge management systems, condition ratings

1. Introduction

In 2013, the American Society for Civil Engineers (ASCE) released an updated Infrastructure Report Card that found nearly 25% of the nation's bridges to be either structurally deficient or functionally obsolete. A bridge is considered structurally deficient (SD) when it is in need of significant maintenance, rehabilitation, or replacement due to deteriorated physical conditions and is considered functionally obsolete (FO) when it does not meet current standards, such as vertical clearances or lane widths. To make these condition assessments, the Federal Highway

Administration uses information from inspection reports that are hosted by state and federal bridge management systems (BMS). BMS are heavily dependent on field inspectors, who collect information on bridge elements and bridge components, evaluate their condition, and enter this data into the BMS database. Among the various tasks of BMS, field inspection is the most essential in evaluating the current condition of steel bridges, which are vulnerable to fatigue-induced damage: the process of material degradation and/or cracking by repeated loads. Fatigue damage occurs over a long period of time and is the primary failure mechanism in steel bridges reaching their original design life [1]. Fatigue damage is largely dependent on the size of the traffic loadings, the frequency of the loads, and the type of detail under examination [2]. The damage usually initiates at the fatigue-prone areas of the bridge: the bridge connections, attachments, and details, such as welds connecting connection plates to steel girders. The defects begin to grow under repetitive loads until a bridge inspector finds the crack in a visual inspection. If the crack is not attended to, it will continue to grow until the structural component is capable of fracture and is also considered to be at the end of its total fatigue life.

Currently, the Federal Highway Administration (FHWA) uses fatigue life estimations to predict the performance of steel bridge members [3]. These fatigue estimates describe the onset of a crack by correlating the magnitude of the stress ranges with the number of load cycles the member has experienced. However, once cracking has occurred, there are no federal or state specifications for crack analysis or crack growth predictions. The fatigue life assessment can be more accurately characterized when crack growth analysis is also included in the assessment. This paper presents a fatigue life assessment method that combines the stress-cycle approach, currently used in AASHTO LRFD Bridge Design Specifications 2014, with a fracture mechanics approach. The damage accumulation results are integrated with current condition state classifications used in BMS.

2. Fatigue life assessment modeling

The fatigue life of a member is the number of load cycles a member can endure before confronting the structure's serviceability limit state. Within a structure's fatigue life, a structure is considered to experience deterioration in two different periods in time: crack initiation and crack propagation. The crack initiation period describes the time when cracks are just beginning to initiate from points of stress concentrations in structural details. Starting with an inclusion in the material, an initial microscopic crack grows a microscopically small amount in size each time a load is applied. The crack initiation period ends when a microscopic crack reaches a predefined critical crack size, typically a crack that is visible in size. The initiation period covers a significant part of the fatigue life. Once a fatigue crack has initiated, applied repeated stresses cause propagation, or growth, of a crack across the section of the member until the member is capable of fracture. The crack propagation period ends when a crack has reached a critical size or final crack size, determined from the material fracture toughness. When a structure has experienced a crack size at the end of the propagation life, the structure is capable of fracture and is also considered to be at the end of its total fatigue life. It is technically significant to consider the crack initiation and crack propagation stages separately because the practical conditions that have a large influence on the crack initiation period are different from the conditions that will influence the crack propagation period [4].

2.1 Fatigue crack initiation period

The crack initiation period corresponds to the onset of a fatigue crack in a component under traffic loads due to an applied stress. To properly account for the dynamic effects in traffic loads, it is necessary to gather a realistic set of data on the stress history that depends upon bridge traffic [5]. This can be accomplished through structural health monitoring (SHM).

2.1.1 Structural evaluation using structural health monitoring

A SHM system gathers real-time measurements of a structure behavior under the effects of varying vehicle weights and their random combinations in multiple lanes. Therefore, the measured strain data reflects the loading conditions in the particular location of the strain gage. SHM methodologies can be divided into two main categories: a statistical/data model-based approach and a physical model-based approach. In the statistical model-based approach, only the measured response of the structure is considered for an assessment, while a physical model-based approach concentrates on the understanding of the structure from its physical model, and a finite element analysis is frequently employed and validated through SHM [6]. In the physical model-based approach, the field measurements verify and validate the finite element models, and a simulation of traffic loads can be used to conduct a structural damage assessment.

To accurately characterize load histories, the content of a measured signal should be summarized and quantified in a meaningful way. The rainflow cycle counting method is recognized as the most accurate way of representing variable amplitude loading [7] and is preferred for statistical analysis of load-time histories, as described in the standard of the American Society for Testing and Materials [8]. Rainflow counting method is advantageous to other range counting methods because it offers realistic counting results while preserving the amplitudes of the acquired stress ranges. As part of the cycle counting process, it is customary to remove small oscillations that are negligible contributors to fatigue damage. Further, the stress ranges caused from smaller vehicles are often considered negligible compared to trucks. This is not only established in *AASHTO Standard Specifications for Highway Bridges* [9], but the NCHRP Report, *Fatigue Evaluation of Steel Bridges* [10], also pays distinct attention to truckloads when estimating fatigue life, stating “the effective stress range shall be estimated as either the measured stress range or a calculated stress range value determined by using a fatigue truck as specified in the AASHTO LRFD Bridge Design Specification 2014 [11].” Because of the significance of truckloads compared with smaller vehicular passages, it is rational to neglect stress cycles below 1 ksi [12].

2.1.2 Bridge global model

Alongside structural health monitoring, a three-dimensional finite element global model can be developed for linear elastic structural analyses. For a typical steel highway bridge, the global model includes the deck, girders, connection plates, and the cross frames to the girders. The global model contains only the main components of the bridge and is primarily used for modal analysis, finding the displacement output of the whole bridge, and critical fatigue location determination known as hotspots, i.e., the locations of known high tensile strength. Field measurements were taken to calibrate the finite element model,

accelerometers were used to capture the bridge frequency, laser sensors and potentiometers were used to measure the dynamic deflection of the bridge, and strain gages were used on connection plates to capture the stresses of bridge components. The simulation of truckloads on the global model will output the stresses of all the components on the bridge.

2.1.3 Global simulation modeling

Global simulation modeling uses a three-dimensional model of a bridge with a traffic simulation to estimate fatigue damage. The fidelity of the fatigue assessment is dependent on the accuracy of the traffic load model and the accuracy of the structural model. Since larger loads (i.e., truckloads) are major contributors to fatigue damage and the global simulation model requires computational complexity, the traffic simulation only considers truck loading data for the fatigue assessment. There are two main components of truckloads to consider: the loading configuration (i.e., axle weights and axle spacing) and the traffic patterns. Weigh stations and traffic monitoring systems are often used by State Transportation Departments to acquire loading configuration and traffic pattern data. This data can be used to develop a traffic load simulation, also referred to as the truckload spectra.

To generate load configuration data, the *Guide Specifications for Fatigue Evaluation of Existing Steel Bridges* [13] recommends collecting data through weigh station measurements. A weigh station is a checkpoint equipped with truck scales. Trucks and commercial vehicles are subject to passing the scales at a very low speed and return to the highway after inspection. Data collected from weigh station measurements includes the number of axles and the axle spacing. The collection of truck traffic data at weigh stations can be used to calculate the effective gross weight of the truck spectra:

$$W = \left(\sum f_i W_i^3 \right)^{1/3} \quad (1)$$

where f_i is the fraction of gross weights within an interval and W_i is the midwidth of the interval.

The traffic patterns are another influence to fatigue damage. The actual traffic flow through a bridge is affected by the traffic on the connecting roadways. Automatic traffic recorders can be used to realistically capture the actual traffic patterns, such as vehicle speed, lane distribution, and vehicle position. Time-varying vehicular count data combined with weigh station measurements are used to develop a probabilistic-based truck simulation model. After obtaining the time-history spectra, the fatigue life and the remaining fatigue life for this detail can be calculated as a function of stress range and number of cycles. Detailed traffic load simulation is reported in a separate companion paper, *Fatigue Assessment of Highway Bridges under Traffic Loading Using Microscopic Traffic Simulation*.

2.1.4 Crack initiation life prediction

The crack initiation period is characterized by the S-N curve. S-N curves are used to relate the stress range (S) vs. number of loading cycles (n_i) and ultimately define the fatigue life of the material. S-N curves comprise the influence of material, the geometry of the local structure, and the surface condition. Failure for the crack initiation period is defined by a crack that is of a critical size. Until the onset of this fatigue crack, the specimen can be characterized by the amount of current fatigue damage in terms of its fatigue life. So, the specimen may be at x% of its fatigue life,

or the specimen can be classified to have $(100 - x)\%$ remaining useful life. This damage may not be visible upon inspection but is still present in the material.

Since the data in S-N curves were developed under constant amplitude cyclic loading, an effective stress range should be calculated to equivalently represent the variable amplitude cyclic loading on bridge structures. The effective stress range for a variable amplitude spectrum is defined as the constant amplitude stress range that would result in the same fatigue life as the variable amplitude spectrum. For steel structures, the root mean cube stress range (Eq. 2) is calculated from a variable amplitude stress range histogram and is used with the constant amplitude S-N curves for fatigue life analyses [14]:

$$S_{re} = \left(\sum \gamma_i S_{ri}^3 \right)^{1/3} \quad (2)$$

where S_{ri} is the midwidth of the i th bar, or interval, in the frequency-of-occurrence histogram, 3 is the reciprocal of the slope in the constant S-N curve, and γ_i is the fraction of stress ranges in that same interval [15].

2.1.5 Damage accumulation: crack initiation period

The damage accumulation of crack initiation period, d_i , is calculated by comparing the effective stress range to the predefined laboratory values of specimens which are used to construct the S-N curve. Thus, the cumulative damage from the crack initiation life is written as a percentage of the fatigue life by dividing the number of current cycles at the effective stress range, N_e , by the number of stress cycles to fatigue failure, N_f :

$$d_i = N_e/N_f (100) \% \text{ damage} \quad (3)$$

2.2 Fatigue crack propagation period

In the crack propagation period, the crack is considered to be a macro-crack and is now growing through the material. The rate of this crack growth is highly dependent on the material type. While the nature of the material cracking is a nonelastic deformation, the region beyond the crack (at the crack tip) experiences a linear elastic stress field under load.

2.2.1 Linear elastic fracture mechanics

Because the stresses at the crack tip are so small in fatigue problems, the plastic zone is limited, and linear elastic fracture mechanics (LEFM) can be used to assess fatigue crack propagation. Paris model is most widely used model in linear elastic fracture mechanics for the prediction of crack growth. In this model, the range of the stress intensity factor is the main factor driving the crack growth with two parameters C and m that reflect the material properties:

$$\frac{da}{dN} = C (\Delta K)^m \quad (4)$$

where a is the initial crack size, N is the number of fatigue loading cycles, C and m are material properties, and ΔK is the stress intensification factor. For a given initial crack size, once the crack growth rate is determined, then the existing crack size can be easily calculated through a summation over crack size increments starting from the known size.

2.2.2 Stress intensity factor

The stress in the local crack tip is described as a function of the applied stress in the form of a stress intensity factor (SIF). SIFs are used to describe the severity of a stress distribution around a crack tip, the rate of crack growth, and the onset of fracture [16]. Even at relatively low loads, there will be a high concentration of stress at the crack tip, and plastic deformation can occur [17]. The simplest form to describe the “intensity” of a stress distribution around a crack tip can be written as

$$K = \beta S \sqrt{\pi a} \quad (5)$$

where S is the remote loading stress, a is the crack length, and β is a dimensionless factor depending on the geometry of the specimen or structural component. One important feature this equation illustrates is that the stress distribution around the crack tip can be described as a linear function.

For many ordinary cases of cracking, the calculations of stress intensification factors for various crack geometries and loading cases have already been computed and can be obtained from previously published literature, e.g., elliptical cracks embedded in very large bodies [4]. However, for cases with more complex geometries, more accurate K values should be independently calculated. Finite element modeling (FEM) offers a variety of techniques and efficient computation and has proven to offer satisfactory results for the stress intensification factors [4]. In finite element models, the crack is treated as an integral part of the structure and can be modeled in as much detail as necessary to accurately reflect the structural load paths, both near and far from the crack tip.

2.2.3 Fracture toughness

When the crack grows to a particular size, the stresses at the crack tip are too high for the material to endure, and fracture takes place. This critical stress intensity value is more often referred to as the fracture toughness, K_{Ic} , where I denotes opening mode and c represents critical. Fracture toughness is a measured material property, just like Poisson’s ratio or Young’s modulus, and is usually measured through standard compact specimens. The fracture toughness is used to describe the ability of an already cracked material to resist fracture or to indicate the sensitivity of the material and the material’s susceptibility to experiencing cracks under loading [4]. Thus, SIFs can be compared with the fracture toughness variables to determine if the crack will propagate and to determine the size of crack a material can endure until fracture [18]. When the applied stress intensity equals or exceeds the material fracture resistance, K_{Ic} , fracture is predicted.

2.2.4 Crack propagation period cumulative damage

Models that predict fatigue crack growth propagation emphasize that crack growth is largely dependent on the cycle-by-cycle process. Prediction models are referred to as interaction models and non-interaction models. Interaction effects imply that the crack growth rate in a particular cycle is also dependent on the load history of the preceding cycles rather than an independent effect from one cycle. A non-interaction prediction model is used if the interaction effects in the variable amplitude history are assumed to be absent. In a non-interaction model, crack growth in each cycle is assumed to be dependent on the severity of the current cycle only and not on the load history in the preceding cycles. While it is expected that a non-interaction model will lead to a more conservative life prediction than models

that account for interaction effects, considering interaction effects account for retardation in crack growth, a non-interaction model can provide quick and useful information about fatigue crack growth behavior, particularly crack growth rates [4]. The non-interaction prediction model leads to a simple numerical summation in Eq. (6), where $\Delta a = da/dN$:

$$a_n = a_0 + \sum_{i=1}^{i=n} \Delta a_i \quad (6)$$

The accumulation of damage for fatigue crack growth models is consequent of the change in crack size, a , where a_0 is the initial crack size, Δa_i is the change in crack size per cycle, and a_n is the updated crack size [4]. Thus, the cumulative damage from the fatigue crack propagation period, d_p , is written as a percentage of the fatigue life by dividing the current crack size, a_n , by the critical crack size at failure, a_{crit} :

$$d_p = \frac{a_n}{a_{crit}} (100) \% \text{ damage} \quad (7)$$

3. Damage prognoses fatigue life

The assessment for the crack initiation period and the assessment for the crack propagation period can be combined to determine a damage prognosis, D_{Total} , for the entire fatigue life:

$$D_{Total} = \begin{cases} \alpha_I d_i, N_e \leq N_f \\ \alpha_I d_i + \alpha_P d_p, N_e > N_f \end{cases} \quad (8)$$

where N_e is the number of cycles the element has currently experienced, N_f is the number of cycles to failure, d_i is obtained from Eq. (3) and d_p is obtained from

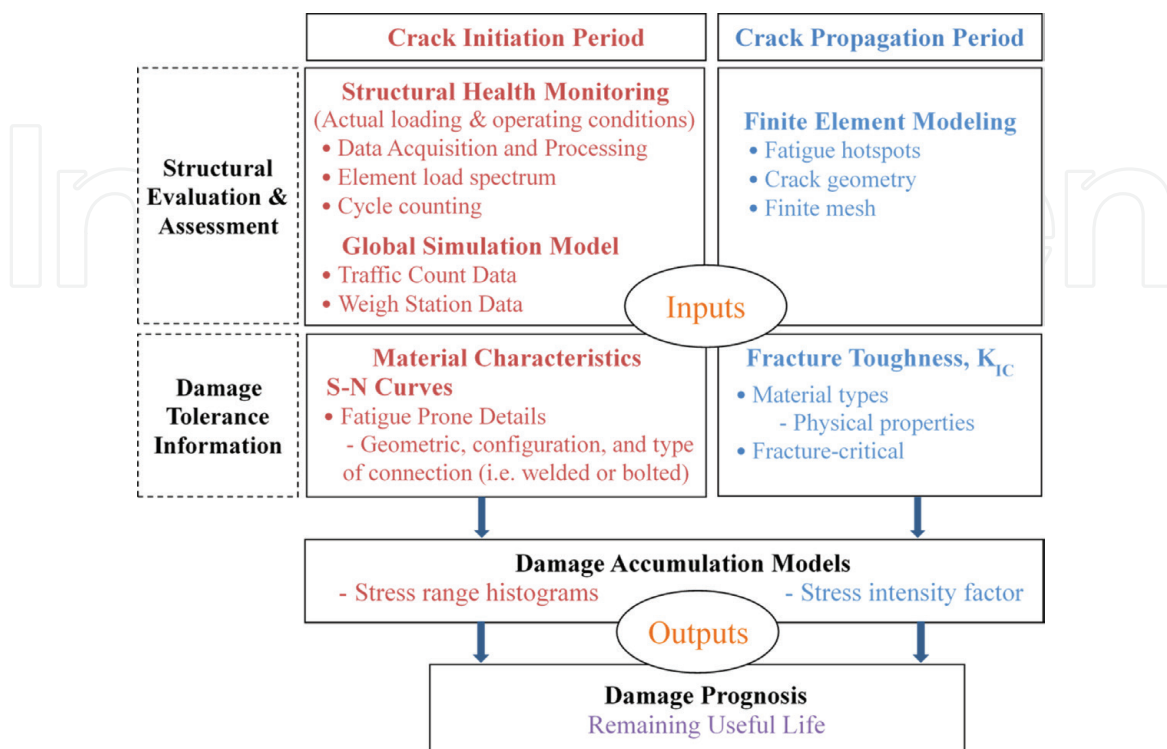


Figure 1.
 Fatigue damage prognoses with structural health monitoring.

Eq. (7), and α_i and α_p are rate adjustment factors since the crack initiation period and crack propagation period are not equal in time. These factors can be altered to reflect the rate of damage. **Figure 1** displays the various aspects of fatigue analyses that are considered in the derivation of a fatigue damage prognosis. The diagram summarizes the analyses that are detailed in the preceding sections of this paper. As seen in the diagram, the damage accumulation model that defines crack initiation is informed by a structural evaluation, which can be conducted by means of a global simulation model that is validated with structural health monitoring. SHM gathers information about the actual load distributions and operating conditions of the bridge components. This information is processed and evaluated with damage tolerance information, which describes the material characteristics and material properties, such as the number of stress cycles a structural element can endure before cracking. The damage accumulation model that defines the crack propagation period is informed by finite element models of fatigue hotspots with existing cracks. The finite element modeling provides insight of the stress rate at the crack tip. Fracture toughness is then used to determine the critical crack size, at which the structure is described to be at the end of its fatigue life. Ultimately, the damage accumulation models in the crack initiation period and crack propagation period are used to determine the structure's damage prognosis (remaining useful life).

3.1 Integration of damage prognosis with bridge management systems

Currently, most US state Departments of Transportation (DOTs) report their bridge inspection findings using AASHTO Pontis software, which poses the guidelines for capturing damage of bridge elements. The conditions of bridge elements are categorized into element condition states to reflect these damages. The AASHTO Pontis software is most useful for state DOTs, since it provides an internal tool for mapping the element condition states back into the national condition ratings.

Table 1 summarizes the four condition states related to fatigue damage. These condition states are found in the *Maryland Pontis Element Data Collection Manual* [19].

The condition states in **Table 1** can be used with the fatigue life curve (**Figure 2**) to gather quantitative information of the fatigue life. An element in condition state one is considered a new element or in "like new" condition; it has no fatigue damage present. This element falls within the early stages of the crack life-initiation period. Condition state two recognizes fatigue damage. This damage could be found from a stress-cycle analysis that showed the structure was nearing the end of the crack initiation life or could be the result of a visual inspection from of a small crack that is not considered to be in immediate need of repair. An element in condition state two will be approaching the critical crack size of the crack initiation period and is merging into the crack propagation period. Thus, an element is in the propagation period in condition state three, which explicitly calls for additional analyses. In many state DOTs, it is suggested that deterioration modeling be used to assess the fatigue damage and evaluate the probability of transitioning from condition states [19]. A stress-cycle history can be used to obtain information about the daily or yearly cycle count and stress ranges on the structure. In the event there is enough information about the crack, crack growth models can be used to obtain information about the crack growth rate. This is particularly important information to obtain if the fatigue damage is on a primary component of the structure. Finally, an element in condition state four is in need of immediate rehabilitation or replacement. Analysis can still be used to understand the problem with this section of the bridge to make appropriate changes and to increase the bridge life.

A description of the national bridge element condition states is described in **Table 1** and is used in parallel with the FHWA Bridge Preservation Guide, which

National bridge element condition states				
Defect	Condition state 1 (good)	Condition state 2 (fair)	Condition state 3 (poor)	Condition state 4 (severe)
Cracking/fatigue	None	Fatigue damage	Fatigue damage (Analysis warranted)	Severe fatigue damage
		Fatigue damage exists but has been repaired or arrested. The element may still be fatigue prone	Fatigue damage exists which is not arrested. Condition state used for first time element is identified with crack	Fatigue damage exists which warrants analysis of the element to ascertain the serviceability of the element or bridge

Table 1.
 Pontis system condition states related to fatigue [19].

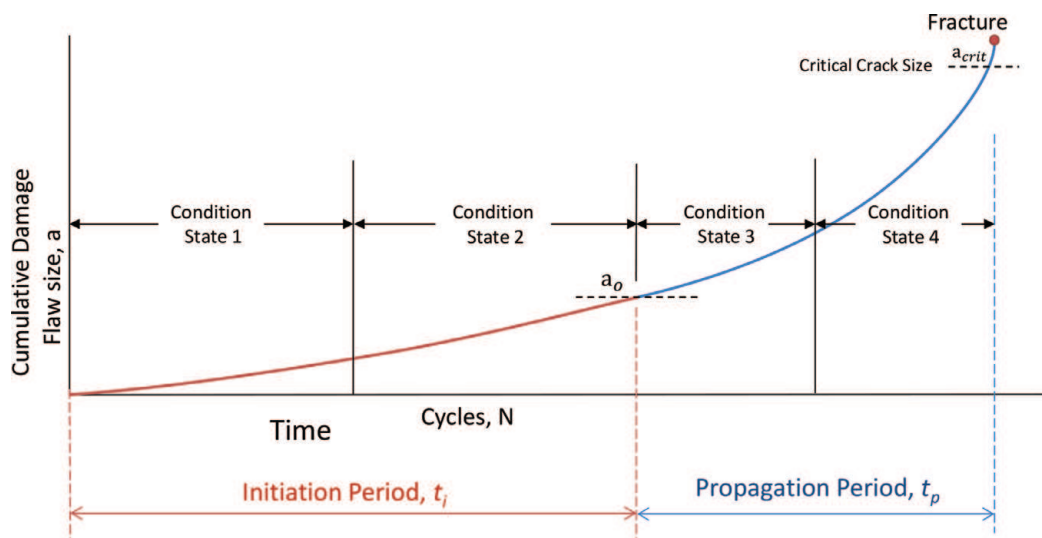


Figure 2.
 BME condition states integrated into fatigue life curve.

hosts the commonly employed feasible actions that inspectors and state DOTs should take, given the condition state of their bridge. The purpose of the FHWA Bridge Preservation Guide is to provide a framework for a preventive maintenance program for bridge owners or agencies [20].

4. Case study

The fatigue assessment in this paper was conducted as part of the University of Maryland project to design and implement an integrated structural health monitoring system that is particularly suited for fatigue detection on highway bridges. Data for the analyses was acquired from a highway bridge carrying traffic from interstate 270 (I-270) over Middlebrook Road in Germantown, MD, seen in **Figure 3**. This bridge is referred to as the Middlebrook Bridge.

The Middlebrook Bridge was built in 1980 and reconstructed in 1991. With help from Maryland bridge inspectors, this bridge was selected as a good candidate for fatigue monitoring due to the average daily truck traffic, the bridge's maintenance



Figure 3.
Maryland bridge carrying I-270 over Middlebrook Road.

history, the geometric configuration, and the identification of existing fatigue cracks on the connection plates.

The Middlebrook Bridge is a composite steel I-girder bridge consisting of 17 welded steel plate girders with a span length of 140 ft. The bridge has three traffic lanes in the southbound roadway and five traffic lanes in the northbound, i.e., a high occupancy vehicle lane, an exit lane, and three travel lanes. Four fatigue cracks were reported in the Maryland State Highway June 2011 Bridge Inspection Report. These four cracks were all found in the welded connections between the lower end of the cross brace connection plate and the girder bottom flange.

The Middlebrook Bridge is built with skewed supports to accommodate the roadway below the bridge. Due to the skewed supports, the corresponding cross frames are also built with skewed angles. The Middlebrook Bridge was built with K-brace cross frame, seen in **Figure 4**.

The skew angle of the cross frames are built to code and are in accordance with AASHTO LRFD Bridge Design Specifications [11], so long as the skew angle is less than 20 degrees. A bridge with skewed cross braces is more prone to fatigue damages because its geometric configuration enhances the live load effects. The connections of the skewed cross braces are bent at an angle to connect with the transverse stiffeners of the bridge girders. When the bridge girders deflect, this angle introduces a bending effect into the transverse stiffeners.



Figure 4.
K-type cross brace on Middlebrook Bridge.

4.1 Structural health monitoring and data processing

A connection plate of a steel girder highway bridge is selected for long-term monitoring, shown in **Figure 5**.

This connection plate was identified by Maryland State Bridge inspectors in 2011 to have an existing active crack, i.e., a crack that is growing in size. The crack was described in inspection reports as "... very fine crack in the weld that connects the web stiffener to the top of the lower flange. The crack runs along the top of the weld material next to the stiffener and begins at the toe of the weld" [21].

Only one strain transducer was used to continue monitoring the bridge in a long-term monitoring evaluation. The strain transducer was placed on one of the stiffeners that showed to high tension stress. The bridge itself is loaded in bending by the dynamic effects caused from the vehicle passage. Specifically, **Figure 6** displays a sample of the acquired stress data as a function of time that was taken from a connection plate. The variation in loading of the load spectrum on the connection plate is dependent on the number of vehicles passing the bridge and the weight of the vehicle. Given that the traffic volumes and patterns are sporadic, the captured bridge loads are also sporadic. Strain data was collected from the bridge over the course of 1 year.

4.2 Fatigue analysis

The acquired variable amplitude strain data is converted to stress for linear damage accumulation models, where stress ranges are the main contributor to fatigue damage. In addition, methods of extrapolation were used to fill in missing points of data. The method of extrapolation that has been applied to the fatigue data is done in the rainflow domain. The results of the extrapolated rainflow matrix were modeled from a measured rainflow history, where the density of rainflow cycles was calculated. The calculation of this density provided the number of stress cycles and stress ranges that were to be estimated for each specific hour of the day. The data was then processed with the rainflow cycle counting method to count the number of stress ranges. **Figure 7** displays a histogram of measured stress ranges. This particular histogram displays the traffic data that was accumulated on the bridge over 8 days.

With variable amplitude stress history, the variable stress cycles are associated with a particular stress range value that will map the measured data with the S-N

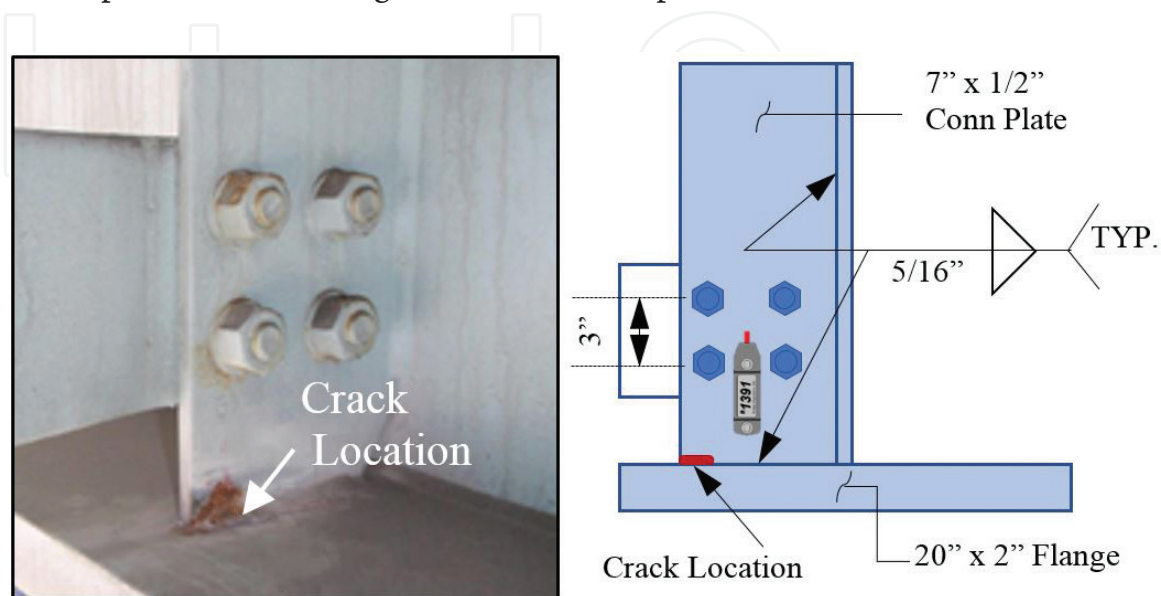


Figure 5. Connection plate with known crack (left) and schematic of strain gage location (right).

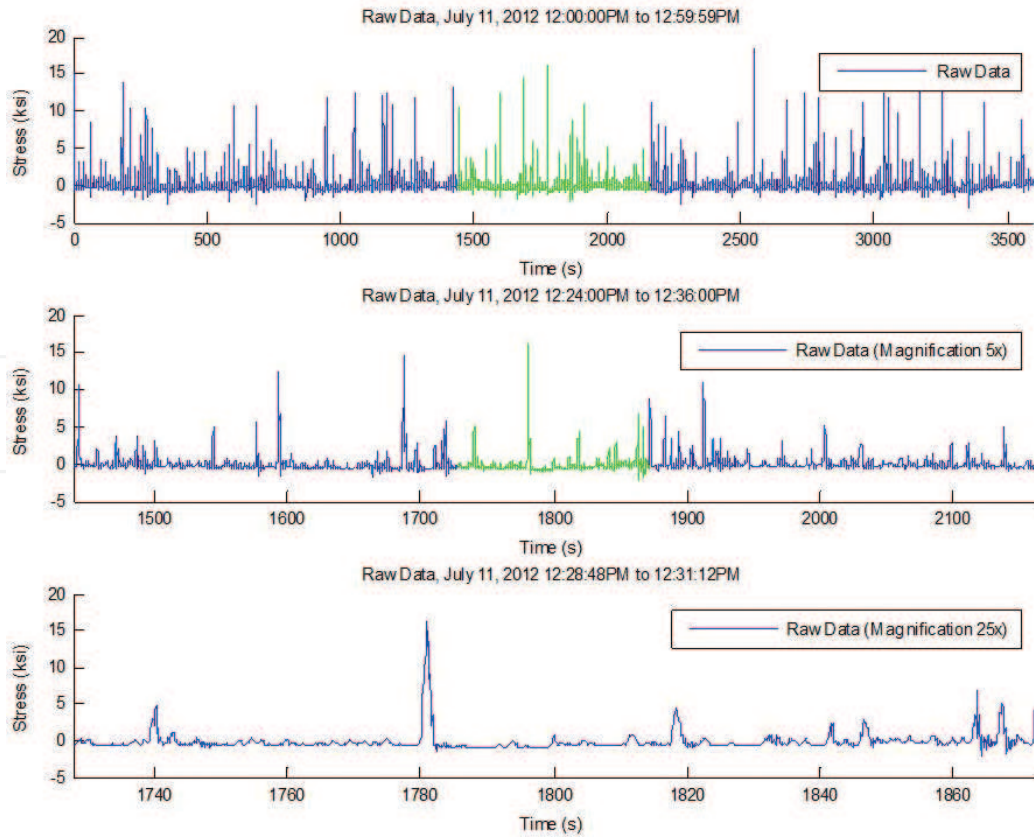


Figure 6.
Illustration of variable amplitude loading.

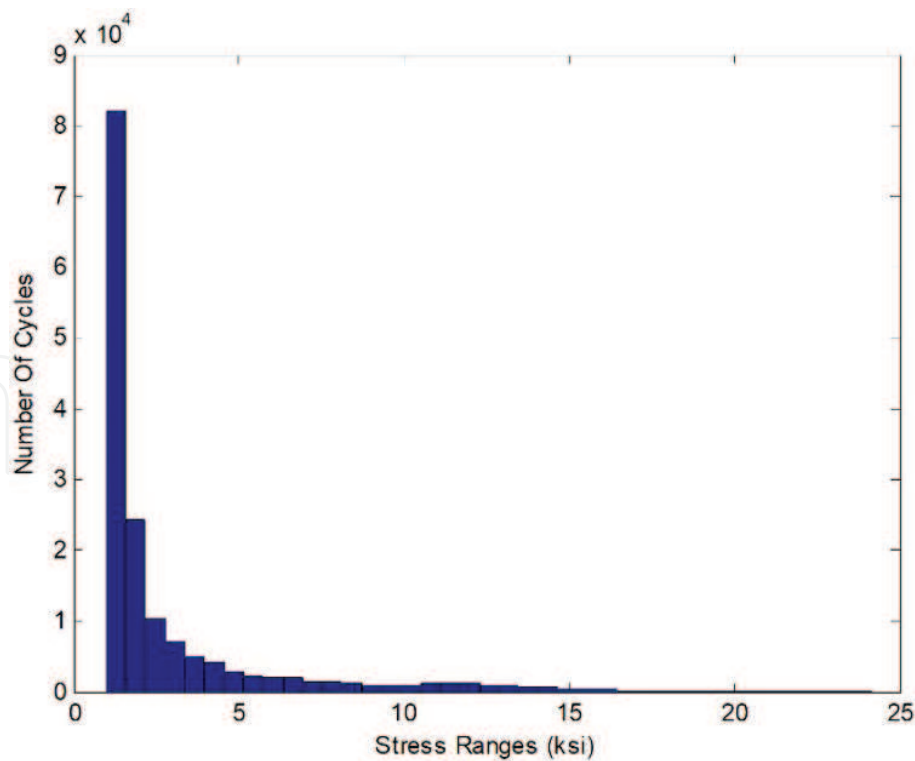


Figure 7.
Histogram of measured stress ranges.

curves. The measured histograms showed an un-proportionally large amount of cycles occur at smaller stress ranges. Therefore the stress ranges are truncated, and an effective stress range is solved for; with S-N curves the number of cycles to

failure is based on the effective stress range. For this case study, the effective stress range (s_{re}) was found to be = 7.2 ksi, and the number of cycles over the course of 1 year were approximately 5.8 million cycles.

In accordance with the histograms for this case study, as the effective stress range increases, the number of stress cycles decreases dramatically. Without including an increase in traffic volumes, the effective stress range and number of cycles are assumed consistent for each year. Under this assumption, the estimated fatigue life for the crack initiation period was 18.0 years. **Figure 8** displays the yearly accumulation until failure is reached on the S-N curve.

4.3 Global model and simulation

A three-dimensional global model of the southbound direction, seen in **Figure 9**, was created to evaluate a bridge's response to loading. The model of the southbound superstructure consisted of eight I-girders. The concrete deck, the eight I-girders, and connection plates which connected cross frames to the girders were modeled by shell elements, while all the cross frames were modeled by spatial frames along their center of gravity. Special link members were defined to connect girder elements and concrete deck elements at the actual spatial points where these members intersect. The translations in the x-, y-, and z-directions were fixed at the abutments to represent the actual characteristics of support and continuity.

To study the dynamic effects of the Middlebrook Bridge, simulated truckloads were applied to the global finite element model through traffic simulation software, Traffic Software Integrated System (TSIS) 6.0. The data that was used to simulate the truckloads were taken from Maryland State Highway Administration's Internet Traffic Monitoring System (ITMS) and a local weigh station that is approximately 10 miles north of the Middlebrook Bridge but on the same interstate [23]. The ITSM features permanent Automatic Traffic Recorders that count traffic continuously throughout the year and breaks down the traffic count data by class, volume, and lane distribution [24]. The average hourly volume varied from 505 to 4215, and the

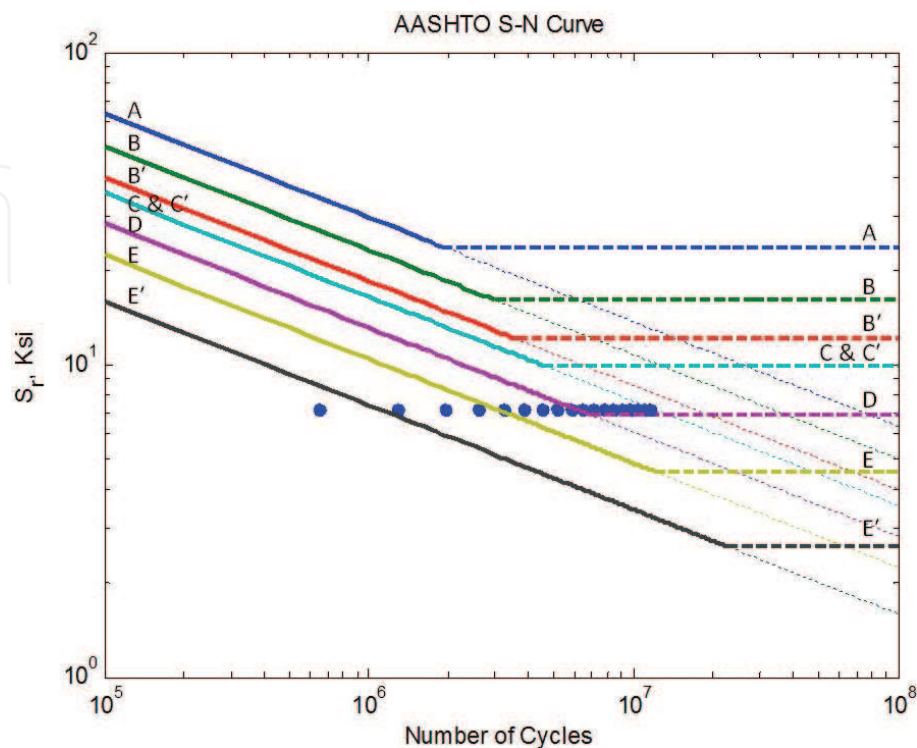


Figure 8.
AASHTO S-N curve with cumulative points plotted until failure.

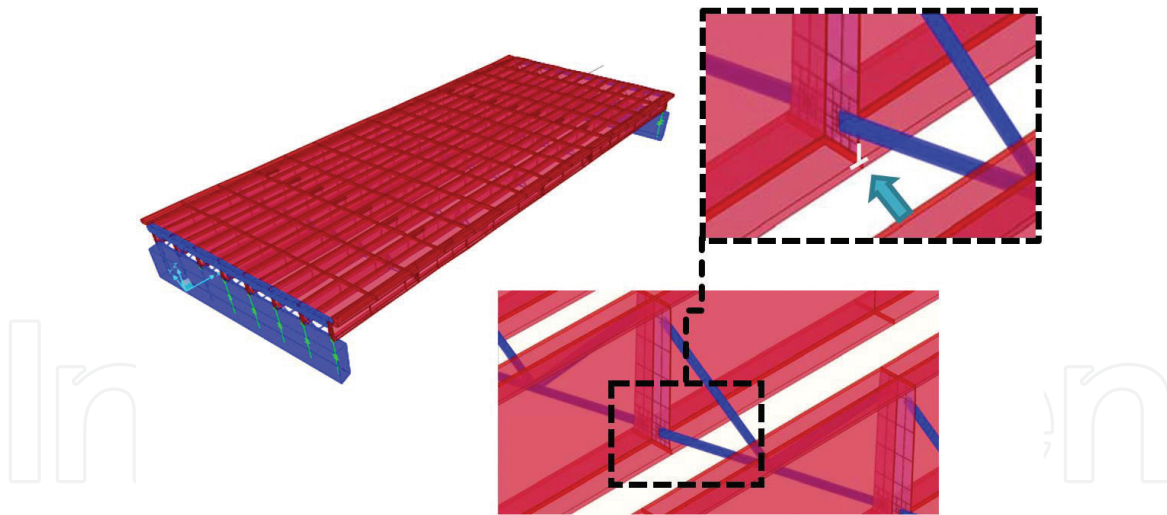


Figure 9. Global model of Middlebrook Bridge and location of local model [22].

truck percentages also varied from about 10.5 to 20%. The weigh station-collected weight data of the truck traffic and the trucks were categorized into seven classes based on the number of axles. The majority of trucks were 2-axle which made up 25% of trucks and 5-axle, which made up 68% of trucks. The simulated truck network contained the mainline section of the highway with the Middlebrook Bridge in the center and adjacent ramps. Three classes of trucks were used for the simulation, shown in **Figure 10**. From the collected data, the simulation included the axle weight, axle spacing, vehicle position, and speed at each time step in the simulation.

The loading data from the simulation matched the loading data from field monitoring, and the simulated truckloads on the global model of the Middlebrook Bridge confirmed high tensile stresses between cross-frame connection plates and girder bottom flanges. These stresses are highest at the outer edge of the connection plate where the existing fatigue crack on the I-270 Bridge over Middlebrook Road was located. More detailed traffic load simulation is reported in a separate companion paper, *Fatigue Assessment of Highway Bridges Under Traffic Loading Using Microscopic Traffic Simulation*.

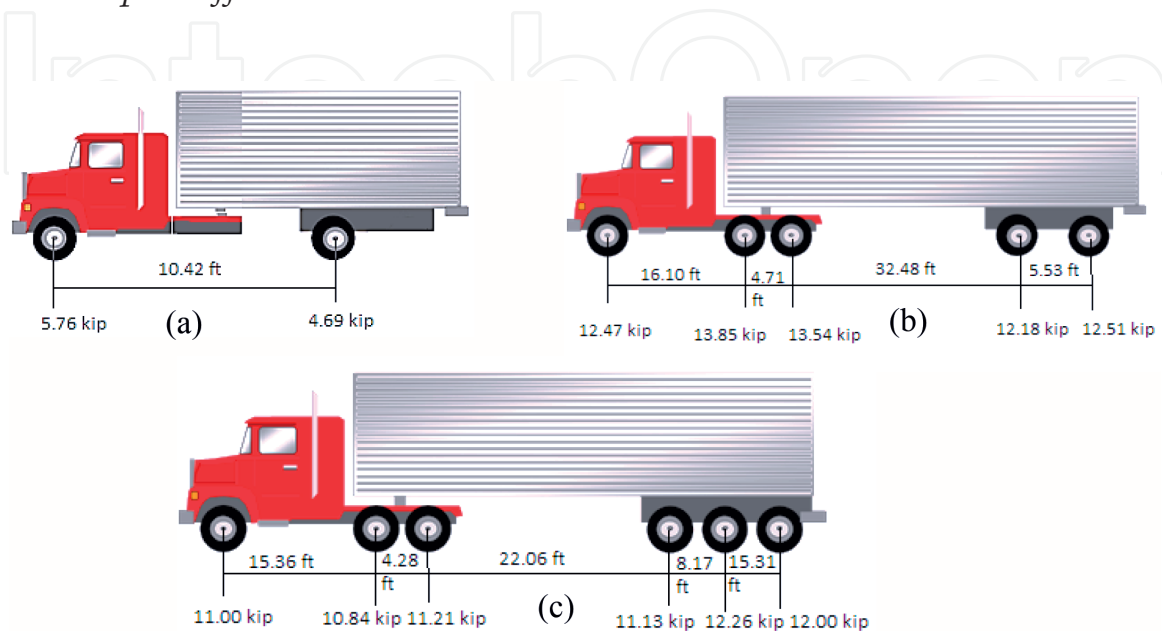


Figure 10. Fatigue truck configurations (a), small truck, (b) medium truck, and (c) large truck.

4.4 Fracture analysis

Since the interest is to obtain a SIF, the global model cannot be any more refined, and a local model of this critical region was created for the purpose of understanding the stress field around the crack. A local model was created by applying the resulting deflections from the global model as resulting displacements in the local model. Since the deflections are a result of simulated traffic loads, applying the deflections simulates the loads transferred across a free-body section of the global model where the local model resides.

Additionally, the stress loads at the location of the strain gage were applied to the local model at the corresponding perimeter location. **Figure 9** displays the location of the local model within the global structure. This location is described with white lines that outline the local model geometry. **Figure 11** displays the local model with applied displacements and forces. A dashed rectangle outlines the location of the existing crack. A fine mesh is created around the previously identified existing crack, and a radial mesh is created around the crack tip. The crack was modeled with an assumed depth of 0.05 inch, which is slightly greater than a largest depth of micro-crack ($0.05 \text{ mm} < a < 1 \text{ mm}$) and approximately the length of the penetration of the fusion in a fillet weld [25]. **Figure 12** displays the stress contour of the y-component of the cross section and a magnified view at the location of the crack.

4.4.1 Damage tolerance and fracture toughness

The specifications of the American Society for Testing and Materials for A572 Grade 50 steel require a minimum yield strength value of 50 ksi. The fracture toughness for the steel on the Middlebrook Bridge is $K_{IC} = 56 \text{ ksi} \sqrt{\text{in}}$. The critical crack length that corresponds to the fracture toughness comes from the fracture mechanics equation for critical SIF. Under the parameters that fit the Middlebrook Bridge, the critical crack size is $a_{crit} = \frac{K_{IC}}{\pi \beta^2 \sigma^2} = .15 \text{ in}$.

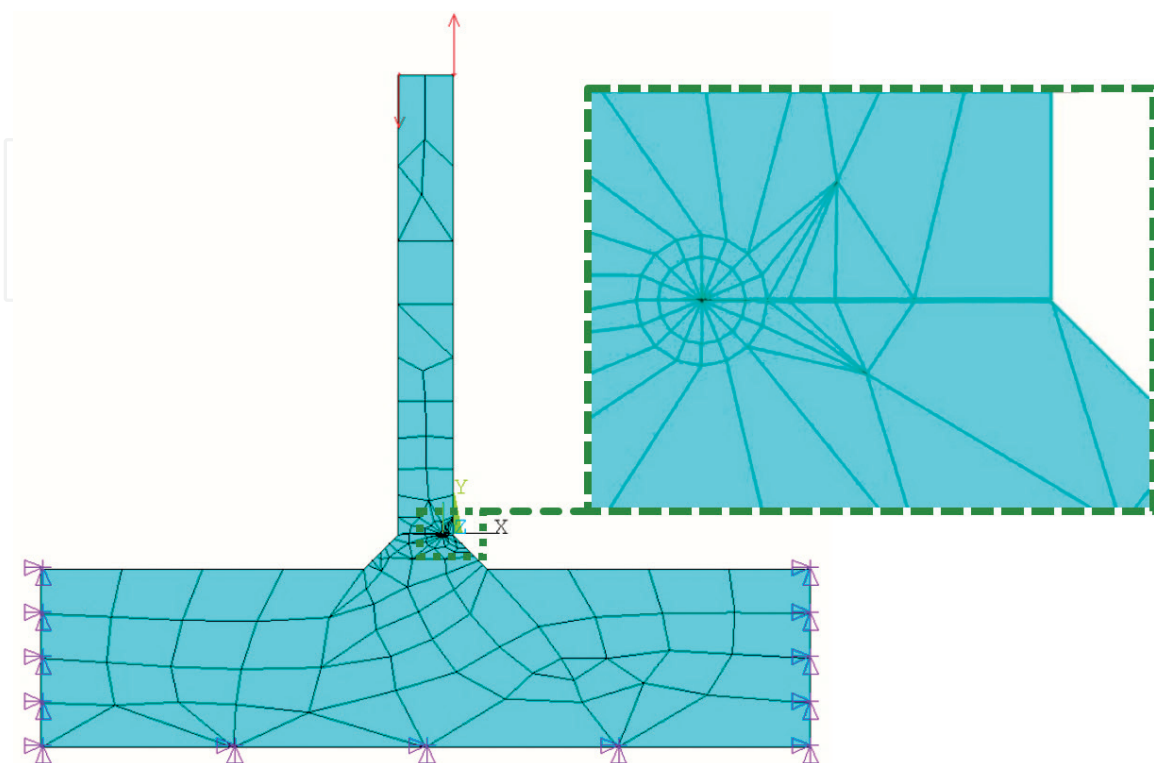


Figure 11.
FEM local model with applied displacements and forces.

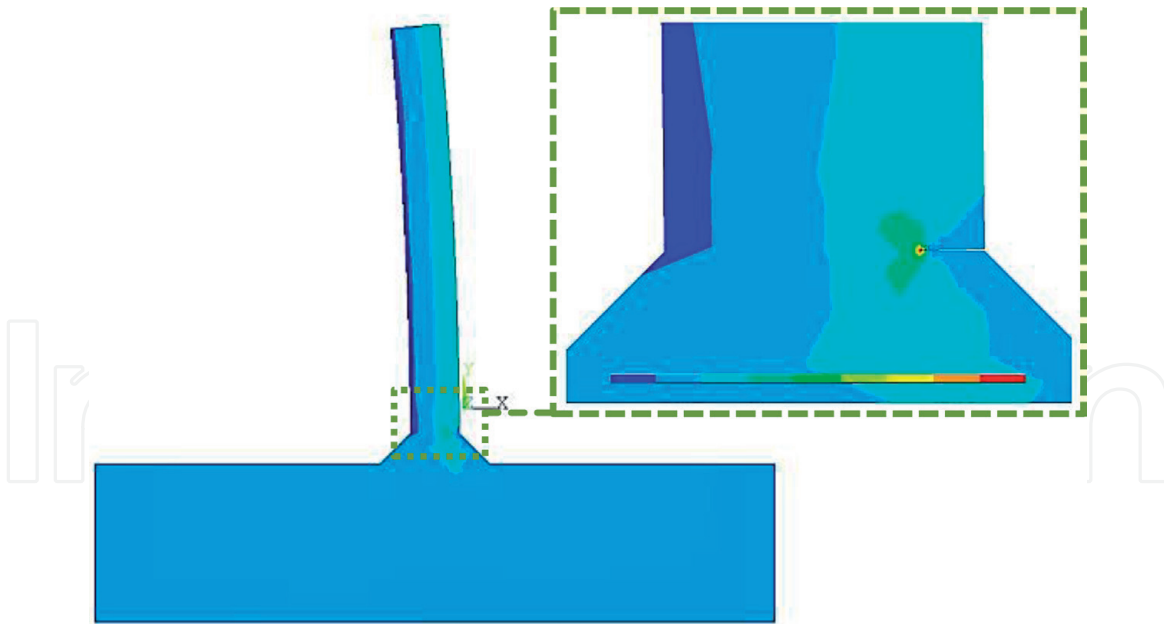


Figure 12.
Stress contour of crack to illustrate plastic zone at crack tip.

4.4.2 Crack growth and total cumulative damage

The computed SIF from the local model was used alongside Paris law to solve for the yearly crack growth rate. Rearranging Eq. (5), the crack size, a , at any given time, is a function of the SIF and the effective stress range. The accumulation of damage for fatigue crack growth models (shown in Eq. 6) is consequent of the change in crack size, Δa_i ; then the crack would reach the critical size after 9.6 years. Since the bridge inspectors first noticed the bridge cracking in 2011, at the time of testing (2012–2013), the crack had been present for about 1–2 years. The crack was repaired in 2014, at which time the remaining useful life for this bridge element was calculated to be 6.6 years to failure.

4.5 Integration of damage with Maryland condition states

The case study was estimated from measured and extrapolated load distributions to assess the life of the bridge. The fatigue life of the crack initiation period was found to be 18 years, and the fatigue life of the crack propagation period was found to be about 9 years. Accordingly, rate adjustment factors were selected to be $\alpha_i = 0.7$ and $\alpha_p = 0.3$. The second row in **Table 2** illustrates the amount of damage for each condition state. The third row is a simplified explanation of the condition states which are found in the *Maryland Pontis Element Data Collection Manual*, and the last row is the feasible actions for these condition states from the FHWA Bridge Preservation Guide.

	Condition state 1	Condition state 2	Condition state 3	Condition state 4
D_{Total}	$0 \rightarrow \frac{1}{2}\alpha_i$	$\frac{1}{2}\alpha_i \rightarrow \alpha_i$	$\alpha_i \rightarrow (\alpha_i + \frac{1}{2}\alpha_p)$	$(\alpha_i + \frac{1}{2}\alpha_p) \rightarrow (\alpha_i + \alpha_p)$
D_{Total} , %	0–35%	35–70%	70–85%	85–100%
Cracking/fatigue	None	Fatigue damage	Analysis warranted	Severe fatigue damage
Feasible action	Do nothing	Preventive maintenance	Rehabilitation	Rehabilitation or replacement

Table 2.
Damage accumulation mapped to bridge condition states.

In 2014, when the crack was repaired, the calculated percent damage was 87.2%, correlating to condition state 4, “Fatigue damage exists which warrants analysis of the element to ascertain the serviceability of the element or bridge.”

5. Summary and conclusions

This paper proposes a damage accumulation model to more accurately characterize fatigue damage prognoses of bridge elements. The fatigue life has been described and divided into two periods: the initiation period and the propagation period. An empirical correlation approach, characterized by the S-N curve, is used to analyze the initiation period, and the data acquired from SHM and traffic simulation models are used to inform the crack initiation analyses. SHM is shown to have a significant contribution in damage prognosis, where the sensing information instrumentation is used to validate FEM models and acquire information about a bridge’s response to loads. It is shown how this data can be particularly useful when processed through cycle counting algorithms, and methods of extrapolation are applied to gather information on stress range distributions to estimate future traffic loads of the bridge. Fatigue damage assessments in the crack initiation period can be supplemented with a fracture mechanics analysis, which defines the crack propagation period and estimates crack growth. It is also shown how finite element modeling can be used to solve for the SIF, which is then used to estimate the growth rate. A case study is presented to illustrate the application of the fatigue damage prognoses on a steel highway bridge element. The damage accumulation models are used to estimate the onset of a fatigue crack and fatigue crack growth rates and ultimately derive a damage prognosis of the bridge element.

Acknowledgements

This research was partially sponsored by the US Department of Transportation’s Office of the Assistant Secretary for Research and Technology (USDOT/OST-R), under The Commercial Remote Sensing and Spatial Information (CRS&SI) Technologies Program. This support is acknowledged and greatly appreciated.

Author details

Timothy Saad¹, Chung C. Fu^{1*}, Gengwen Zhao² and Chaoran Xu¹

¹ The Bridge Engineering Software and Technology (BEST) Center, Department of Civil and Environmental Engineering, University of Maryland, College Park, MD, USA

² Virginia Department of Transportation, Richmond, VA, USA

*Address all correspondence to: ccfu@umd.edu

IntechOpen

© 2018 The Author(s). Licensee IntechOpen. This chapter is distributed under the terms of the Creative Commons Attribution License (<http://creativecommons.org/licenses/by/3.0>), which permits unrestricted use, distribution, and reproduction in any medium, provided the original work is properly cited. 

References

- [1] FHWA. Focus Accelerating Infrastructure Innovations. Federal Highway Administration Launches Steel Bridge Testing Program. 2011
- [2] Haldipur P, Jalinoos F. Detection and Characterization of Fatigue Cracks in Steel Bridges. 2010. Available from: www.structuralfaultsandrepair.com
- [3] FHWA. Bridge Inspector's Reference Manual. Vol. 2. Washington DC: FHWA NHI Publication No. 12-050; 2012
- [4] Schijve J. Fatigue of Structures and Materials. 2nd ed. Netherlands: Springer Science+Business Media B.V.; 2009
- [5] Mohammadi J, Guralnick SA, Polepeddi R. Bridge fatigue life estimation from field data. Practice Periodical on Structural Design and Construction. 1998;3(3):128-133
- [6] Zhou YL, Maia NM, Sampaio RP, Wahab MA. Structural damage detection using transmissibility together with hierarchical clustering analysis and similarity measure. Structural Health Monitoring. Sage Publication. 2017;16(6):711-731. Available from: https://www.nafems.org/downloads/FENet_Meetings/Trieste_Italy_Sep_2002/FENET_Trieste_Sept2002_DLE_Zafosnik.pdf/
- [7] Shantz CR. Uncertainty Quantification in Crack Growth Modeling Under Multi-Axial Variable Amplitude Loading. Nashville, Tennessee: Graduate School of Vanderbilt University; 2010
- [8] ASTM E-1049. Standard Practices for Cycle Counting in Fatigue Analysis. West Conshohocken: ASTM International; 2011
- [9] AASHTO. Standard Specifications for Highway Bridges. Washington, D.C.: American Association of State Highway and Transportation Officials. 2002
- [10] NCHRP. Fatigue Evaluation of Steel Bridges. Washington, D.C.: National Academy of Sciences, Transportation Research Board. 2012
- [11] AASHTO. LRFD Bridge Design Specifications. 7th ed. Washington DC: American Association of State Highway and Transportation Officials. 2014
- [12] Massarelli PJ, Baber TT. Fatigue Reliability of Steel Highway Bridge Details. US DOT FHWA, Charlottesville, Virginia: Virginia Transportation Research Council; Virginia DOT. 2001
- [13] AASHTO. Guide Specifications for Fatigue Evaluation of Existing Steel Bridges. Washington DC: American Association of State Highway and Transportation Officials; 1990
- [14] Zhou YE. Assessment of bridge remaining fatigue life through field strain measurement. Journal of Bridge Engineering. 2006;11(6):737-744
- [15] Keating PB, Fisher JW. Fatigue Tests and Design Criteria. Bethlehem, PA: National Cooperative Highway Research Program and Fritz Engineering Laboratory; 1986
- [16] Zafosnik B, Ren Z, Ulbin M, Flaker J. Evaluation of stress intensity factors using finite elements. FENet: A NAFEMS Project; 2002
- [17] Mertz D. Steel Bridge Design Handbook: Design for Fatigue. Washington, D.C.: FHWA-IF-12-052-Vol.12; 2012
- [18] CAE Associates. Fracture Mechanics in Workbench v14.5 ANSYS e-Learning Session. Middlebury. 2013

[19] MDSHA. Pontis Element Data Collection Manual. Baltimore, MD: Bridge Inspection and Remedial Engineering Division, Office of Bridge Development; 2003

[20] FHWA. Bridge Preservation Guide. U.S. Department of Transportation Federal Highway Administration. New Jersey Avenue, SE Washington, DC. 2011

[21] MDSHA. Maryland State Highway Administration Bridge Inspection Report. MDSHA, Maryland State Highway Administration. North Calvert Street, Baltimore, Maryland. 2013

[22] Fu CC, Wang S. Computational Analysis and Design of Bridge Structures. Boca Raton, FL: CRC Press Taylor and Francis Group; 2014

[23] SHA. Internet Traffic Monitoring System. Maryland State Highway Administration. 29 July 2015. [Online]. Available from: http://shagbhisdatt.mdot.state.md.us/ITMS_Public/default.aspx

[24] Zhao G. Truck Loading Simulation for the Fatigue Assessment of Steel Highway Bridges. College Park: University of Maryland; 2015

[25] Janosch J. Investigation into the Fatigue Strength of Fillet Welded Assemblies of E-36-4 Steel as a Function of the Penetration of the Weld Subjected to Tensile and Bending Loads. 1993